Life Cycle Assessment of Sodium-Nickel-Chloride Batteries

Malina Nikolic[1], Nora Schelte[1(✉)], Michele Velenderic[2], Frederick Adjei[1], and Semih Severengiz[1]

[1] Sustainable Technologies Laboratory, Bochum University of Applied Sciences, Bochum, Germany
nora.schelte@rub.de
[2] Green Power Brains, Munich, Germany

Abstract. Battery storage systems are a crucial factor for the decarbonization of energy systems, to balance the fluctuating energy generation of renewable energy sources. However, some battery types have disadvantages regarding their environmental impact, due to their material composition. Recently, sodium-nickel-chloride ($NaNiCl_2$) batteries are considered for a wider range of application, especially for off-grid storage applications.

$NaNiCl_2$ batteries offer several advantages: Due to the ceramic electrolyte the battery has no electrochemical self-discharge. The batteries have a high tolerance toward overcharging and deep discharging. The materials are not as expensive and rare as materials for alternative battery types. Manufacturers state that both discharge and charge operations are nearly independent of outside temperature. Furthermore, the batteries are expected to have a lifetime of more than 15 years or 4,500 charging cycles. However, when in stand-by, the battery still needs a stable temperature between 250 °C and 320 °C, to keep the electrodes in a molten state. This is leading to a certain self-discharge, limiting the feasible applications of the battery.

Facing these benefits and downsides of $NaNiCl_2$ batteries, this paper aims to analyse their ecological impacts based on a Life Cycle Assessment using the example of greenhouse gas (GHG) emissions. It addresses the research question whether $NaNiCl_2$ batteries offer advantages compared to alternative battery types, such as lithium-ion and lead-acid. The assessment is based on the analysis of a Bill-of-Materials and implemented for the use-case of a solar mini grid in Tema, Ghana. It considers two scenarios each regarding end-of-life (EoL) and battery lifetime. Depending on the scenario, the GHG emissions of the $NaNiCl_2$ battery amount to 9.1 – 22.7 g CO_2eq per kWh discharged and consumed, compared to 31.3 g CO_2eq for lithium-ion and 122.1 g CO_2eq for lead-acid batteries. The GHG emissions of the whole mini grid are decreased by 32%, if $NaNiCl_2$ batteries are implemented, compared to a mini grid configuration based on a mix of $NaNiCl_2$, lead-acid and lithium-ion batteries.

Keywords: Sodium-nickel-chloride battery · Mini grid applications · Life Cycle Assessment

P. Schossig et al. (Eds.): IRES 2022, AHE 16, pp. 336–362, 2023.
https://doi.org/10.2991/978-94-6463-156-2_23

1 Introduction

To limit global warming to a maximum of 2 °C, it is fundamental to achieve zero-emission energy generation by the middle of the century [1]. Even if the expansion of renewable energies is not on the path to achieve net zero emissions by 2050, the expansion is progressing faster than ever before. Another historically significant increase is expected for the coming years [2]. The use of battery storage systems is unavoidable to achieve a full transition to renewable energies, especially in off-grid or mini grid applications, as they ensure an uninterrupted power supply, balancing the fluctuations of electricity generation from renewable sources.

The application of batteries in solar-powered mini grids is particularly interesting for the Sub-Saharan Africa region [3], as further described in the Sect. 2. Mini grids can be defined as decentralized energy systems, consisting of a set of electricity generators, which are supplemented by further technical equipment, storage capacities and distributing infrastructure. They cover the electricity demand of a certain defined local group [4, 5]. Battery storage systems enable intermediate storage of energy. Thus fluctuations in energy generation from renewables can be balanced out and the demand can be met even in the case of changing weather conditions [6]. They consist of different components; including the battery, monitoring and control systems and power conversion systems [6, 7].

The battery storage systems predominantly used today - lithium-ion (li-ion) and lead-acid batteries - are often criticized in terms of their negative environmental impact (ref. Section 2). Even though the pioneer of today's sodium-nickel-chloride battery was developed already back in 1975, it did not achieve a mainstream breakthrough until being manufactured for industrial applications in 2006 by MES-DEA in Switzerland [8, 9]. However, it holds high potential to be relevant in a future with scarce and increasingly expensive resources, due to its abundant and low-cost component materials [8]. Moreover, the battery is characterized by its non-flammable, safe and recyclable composition [10]. Unlike other battery types, the $NaNiCl_2$ battery is characterized by a high tolerance toward overcharging and deep discharging. Furthermore, charge and discharge are independent of the outside temperature, facilitating use-cases at higher temperatures [11]. As the battery is kept at temperatures above 250 °C, additional energy is needed for self-heating, lowering the overall energy efficiency in stand-by [12].

With the increasing demand for energy storage systems, research in the field of $NaNiCl_2$ batteries is growing at pace. In 2014 a Life Cycle Assessment (LCA) on $NaNiCl_2$ batteries was conducted by Longo et al. [13]. It was followed by a cradle-to-gate LCA on the cell design of $NaNiCl_2$ batteries, comparing planar and tubular cell designs, making recommendations for eco design [14]. There have been some investigations in terms of electric vehicles, comparing $NaNiCl_2$ batteries with different battery types [15]. However, operations and EoL of $NaNiCl_2$ batteries was not in the focus of previous studies or even excluded, e.g. by Longo et al. in 2021 [14]. Their previous study from 2013 [13] included the operation of a $NaNiCl_2$ battery but was not considering waste management, as a meta-analysis of existing LCA of battery technologies studies points out [16]. Furthermore, the potential of using $NaNiCl_2$ battery in off-grid applications in Sub-Sahara Africa has – as far as known – not yet been explored.

This paper analyses the environmental impact of a $NaNiCl_2$ battery, comparing the results with of li-ion and lead-acid batteries. It also includes the use-phase and the EoL, taking a cradle-to-grave approach. Secondly, the paper evaluates the potential environmental impact for the use-case of the "Don Bosco mini grid" in Tema, Ghana, considering the energy demand for cooling or self-heating different battery types. The environmental analysis and optimization of the Don Bosco mini grid is part of the "MoNaL" project, funded by the German Federal Ministry for the Environment, Nature Conservation, Nuclear Safety and Consumer Protection.

The paper is structured as followed: First, it presents the state of the art regarding $NaNiCl_2$ battery systems as well as the environmental impact and recycling of different battery technologies. In addition, the use-case of the Don Bosco mini grid and its previous research is introduced. Afterwards, a LCA of the $NaNiCl_2$ battery is conducted. It measures the Global Warming Potential over 100 years (GWP_{100}), comparing the results with li-ion and lead-acid batteries. Moreover, the application of the $NaNiCl_2$ batteries in the Don Bosco mini grid in Tema, Ghana, is simulated by using a *Generic Modell GHG-LCA Modell of a smart Mini Grid* [17] and compared to the current use of li-ion and lead-acid batteries.

2 State of the Art

$NaNiCl_2$ Battery

The $NaNiCl_2$ battery is also known as ZEBRA (Zero Emission Battery Research Activities) battery [18]. Electrochemical reactions enable the battery to be charged and discharged [11].

As indicated by the manufacturer, the considered battery has a usable capacity of 41 kilowatt-hours (kWh) and is composed of 140 tubular designed battery cells. The battery has a modular design, which can be expanded with additional storage capacity for larger scale applications. Figure 1 shows the modular structure of the battery. The battery container consists of a frame of stainless steel with an insulation layer and a ventilator. The module is placed inside the battery container. Besides the battery cells, the module contains a battery management system (BMS), a heater, a frame - which includes a positive and a negative terminal - and an additional insulation layer. The insulation layers and the heater are essential to heat the battery cells to their operating temperature of 250 °C to 320 °C. These numbers refer to the application in mini grids. For further use-cases, the temperatures are slightly higher, as indicated in most literature [11].

To better understand the electrochemical reaction and thus the charging process as well as the structure of the battery, a schematic composition of a single battery cell is illustrated in Fig. 2. It represents the positive outside design. The cells may be designed with the positive and negative poles reversed. Since this does not affect the LCA, only one option is listed here. The considered battery cells are tubular designed cells. Enclosed by a housing (negative pol), the cell is composed of the following key elements:

- A negative electrode (anode), consisting of sodium (Na),

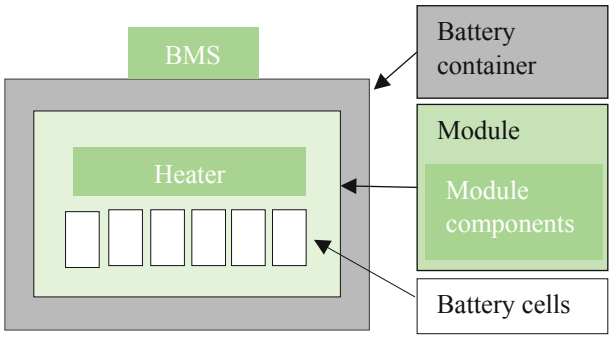

Fig. 1. Structure of the analysed $NaNiCl_2$ battery (Illustration based on manufacturer information and Hesse et al. [7]).

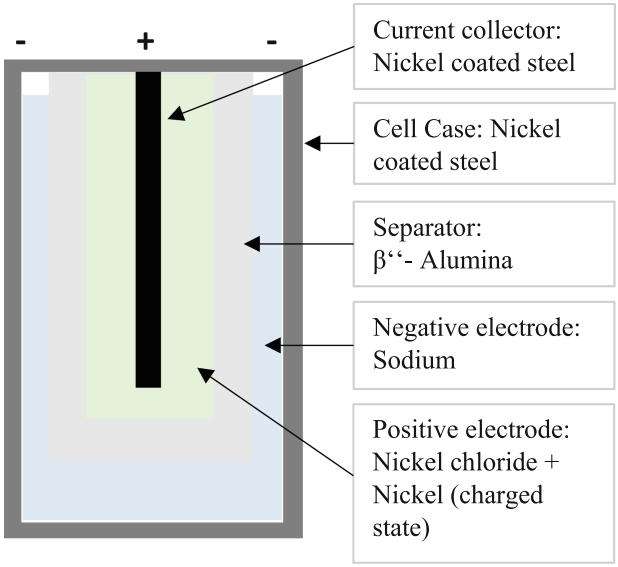

Fig. 2. Tubular designed $NaNiCl_2$ battery cell (Illustration based on EASE [11], Sakaebe [18] and Dustmann [19] and adapted to manufacturer information).

- a positive electrode (cathode) of nickel chloride ($NiCl_2$), nickel (Ni) and sodium aluminium chloride ($NaAlCl_4$) as a liquid electrolyte
- a separator and electrolyte of β‘‘- Alumina (Al_2O_3),
- and a current collector (negative pol) made of nickel coated steel.

At operating temperatures between 250 °C and 320 °C, the $NaAlCl_4$ and Na are liquid and thus the electrodes are in a molten state [11]. Furthermore, the separator reaches a sufficiently high conductivity for sodium ions [20]. Charging the battery requires an endothermic redox reaction and therefore high temperatures. The chemical reactions of charging and discharging processes can be illustrated as in Fig. 3.

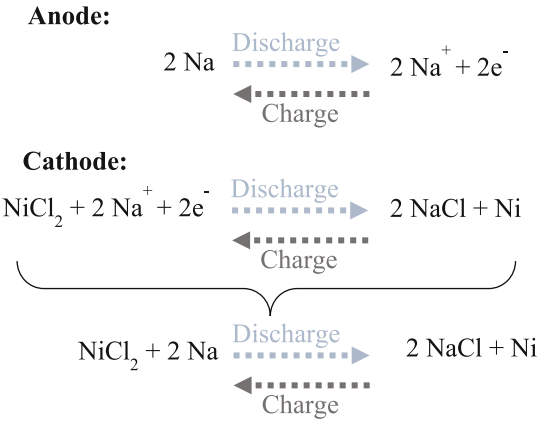

Fig. 3. Electrochemical redox reaction, charging and discharging of the battery (Illustration based on Sakaebe [18] and [20]).

To generate the energy required for the endothermic reaction, i.e. to heat the battery cell to operating temperature and maintain it, some of the charged electricity is directly used by the installed heater. Since the scope of the paper is specifically about the application of $NaNiCl_2$ batteries in a mini grid for storing electricity from photovoltaic (PV) systems, we consider the use-case of charging process during the day and discharging after sunset. This is further described in the section *Use-Case: Don Bosco mini grid in Tema.*

The total efficiency of the battery - including the electricity for self-heating – is, as specified by the manufacturer, at about 85%. It is therefore assumed that about 7.5% energy loss occurs during charging and 7.5% energy loss during discharging. The loss, which occurs when the battery is discharged, has already been subtracted from the overall capacity stated by the manufacturer. Hence, the usable capacity is 41 kWh. According to the manufacturer, the battery still has about 80% of its capacity at the end of its lifetime. It is assumed, that the battery has 100% capacity at the beginning, 80% at the end of its lifetime, losing capacity linearly over time. The capacity loss factor is therefore 90%, resulting in a life cycle usable capacity of 36.9 kWh.

Environmental Impact and Recycling of Different Battery Technologies

Under the current paradigm of sustainable development, end-of-life management forms a crucial part of product design with a thought to the economic and ecological benefits of secondary processes and material recouping [21]. Batteries generally have fallen prey to the situation where disruptive technologies with multiple use-cases and high growth rate in terms of market capture can become an environmental issue, if it has not been designed with the facilities and technologies needed for recycling in mind [21].

In the case of li-ion batteries, their production requires the use of toxic and rare earth materials [22]. Toxic gas emissions, which are released in the case of damage or fire, are hazardous to human health [23]–[25], making recycling or reuse of components very complex. Li-ion batteries cannot withstand large temperature fluctuations and suffer

from high heat, which shortens their lifetime [22, 26]. The recycling of li-ion batteries is hampered not necessarily by technology but rather by low collection rates [21].

The lead-acid battery - whose market dominance is being replaced by li-ion and in the future by $NaNiCl_2$ batteries due to its poor relative energy and power density - is still the most dominant battery used in Ghana and thus merits examination. The EoL management is complicated due to the increased air pollution in lead-acid battery recycling plants [27]. Moreover, it poses risks to human health when processed in an informal manner as it is the case in Ghana [28] [29]. However, recycling processes for lead-acid batteries are well known with recycling rates reaching 100% in developed economies [30]. To recycle a lead-acid battery, the case is crushed, allowing the sulphuric acid electrolyte to escape. The lead electrodes are separated from the polypropylene casing and separated by density. The lead is smelted, and the polypropylene can be reused in new casings. It is economical to do so, due to the relatively high cost of lead. The process is efficient due to the uniformity of the materials used and battery design [30, 31].

As mentioned earlier, the use of $NaNiCl_2$ batteries is enhanced by the global availability of raw materials, which are by themselves non-hazardous [32]. However, batteries in operation contain molten sodium, which poses a significant environmental risk [32]. Recycling processes for the recovery of materials from $NaNiCl_2$ batteries are mainly metallurgical in nature [32, 33]. Full recycling is possible and has been demonstrated in practise with the resultant extraction of iron and nickel. As the required metallurgical process steps are used in steel industry, the recycling can be performed by the next local steel plant. Therefore, EoL treatment of $NaNiCl_2$ energy storage devices is basically collection, dismantling and transporting of components/waste streams to the next steel processing facilities.

Although several recycling facilities exist in Ghana, few to none have the distinct certification to conduct recycling activities; most are certified for the collection and dismantling of e-waste [28]. It must be noted, however, that most e-waste is locally treated by the informal sector through unapproved extraction methods, such as burning and hand-dismantling. Less valuable components, which means locals do not have access to a ready market, are landfilled. It therefore comes down to the implementation of a structured collection system, technology and environmental policies, to enable Ghana achieve high levels of battery recycling [21, 28].

Use-Case: Don Bosco Mini Grid in Tema

In Ghana, 14.1% of the population had no access to electricity in 2020 [34] and access to electricity did not guarantee a constant supply [35]. The electricity generation is mostly based on fossil fuels, as 62% of the electricity from the national grid is generated by oil and natural gas [36]. Diesel generators are as well widely used [35]. Off-grid solutions, such as mini grids which are supplied by renewable energy, can satisfy the increasing demand for electricity and ensure a low-emission and reliable power supply [37] [38].

The Don Bosco mini grid provides energy for the campus of the Don Bosco Renewable Energy Center in Tema, Ghana. The mini grid consists of five individual solar power systems with different types of batteries installed on separate buildings on the campus. These power systems are connected with a private three-phase distribution grid, enabling them to inject and use energy from the mini grid as needed. The mini grid regulates its

frequency on its own and is independent from the Ghana national grid. It is possible to use energy from the national grid to charge the batteries of the mini grid.

The overall installed nominal battery capacity in the mini grid is 394.6 kWh. The mini grid locations, their battery types and capacities are listed in the Table 1.

The nominal battery capacities of the installed lead-acid batteries are given for a discharge time of 100 h and a discharge rate of C100. In solar applications, a discharge in one night, thus a discharge rate of about C10 is common. Longer discharge rates and higher autonomies are possible but often not used, due to the financial constraints caused by oversizing the battery. Furthermore, the maximal depth of discharge (DoD) of a battery must be taken into consideration, which further reduces the life cycle usable capacity of a battery. In the Don Bosco mini grid, maximal DoDs of 90% are set for li-ion and $NaNiCl_2$ batteries, while a maximal DoD of 50% is set for lead-acid batteries. The $NaNiCl_2$ battery, which is installed in in the mini grid, is a different model than the one considered in the LCA.

Considering a discharge rate of 10 h (C10) and the mentioned DoDs, the batteries in the Don Bosco mini grid result in a total usable capacity of 233.34 kWh. However, the installed li-ion batteries ($LiFePO_4$) must be cooled. The electricity demand is 13.05 kWh per day. These efficiency losses are subtracted from the available capacity; thus, a total of 220.29 kWh usable battery capacity is available.

In a previous paper, Stinder et al. [17] generated a generic LCA to design mini grids as environmentally friendly as possible in terms of its GHG emissions. The result is an Excel-based tool in which the user can scale different mini grid configurations. The scalable parameters of the tool include battery type, number of batteries, number of other components (e.g. inverter, PV modules, cable), component lifetime and power output. The tool calculates the life cycle GHG emissions of the whole mini grid per consumed kilowatt hour of electricity. It considers emission factors for li-ion and lead-acid batteries

Table 1. Mini grid locations, battery types and capacities.

Installation	Battery type	Nominal battery capacity @ C100 [kWh]	Usable battery capacity @ C10 [kWh]	Maximal depth of discharge [%]	Life cycle usable battery capacity [kWh]	Lifetime [charging cycles]
Power room	Lead-acid	174.72	131.52	50	65.76	1,500
Chapel	Lead-acid	58.08	43.92	50	21.96	1,500
Provincial house	Li-ion	30.80	30.80	90	27.72	3,000
Provincial house	$NaNiCl_2$	38.60	38.60	90	34.74	3,500
Hostel	Li-ion	30.80	30.80	90	27.72	3,000
Canteen	Li-ion	61.60	61.60	90	55.44	3,000
Total		394.00	337.24		233.34	

of 84 kg CO_2eq and 69 kg CO_2eq per kWh nominal battery capacity respectively. The paper applied the tool in a case-study of a former configuration of the Don Bosco mini grid including 72 lead-acid batteries.

3 Methodology

To measure and analyse the ecological impact of $NaNiCl_2$ batteries along their life cycle, we conduct a Life Cycle Assessment of a $NaNiCl_2$ battery. The LCA is based on the international ISO standards 14040 and 14044. Thereby, the LCA must include the following stages: definition of goal and scope, life cycle inventory, impact assessment and interpretation [39, 40].

Goal and Scope

The goal of the study is to analyse the ecological impact of $NaNiCl_2$ batteries. In a next step, the results shall be compared with li-ion and lead-acid batteries and their application in the mini grid in Tema. Therefore, a cradle-to-grave analysis was conducted; including the life cycle phases production, transport, use-phase and EoL.

Figure 4 illustrates the system boundaries of the LCA. The production phase is divided into the manufacturing of materials (primary materials and energy are used) and on-site manufacturing and assembly of the battery, where electricity is used. This is followed by transportation, use phase and EoL. All steps produce emissions and require energy as an input.

To investigate whether $NaNiCl_2$ batteries have the potential to contribute to zero-emission energy generation, the impact on global warming is particulary interesting. Thus, the considered impact category is the Global Warming Potential over 100 years (GWP_{100}), measured – as defined by the IPCC - in carbon dioxide equivalents (CO_2eq) [41].

We reflect different functional units. Firstly, we consider one kWh of battery capacity, where we relate the life cycle environmental impact of battery production, transport and EoL to both, the nominal capacity and the life cycle usable battery capacity. The life cycle usable capacity reflects efficiency losses due to heating and cooling as well as capacity losses due to DoD and aging. Secondly, we consider one kWh consumed, indicating one kWh of electricity output, which is discharged from the battery and consumed. The life cycle environmental impact is related to the electricity output over lifetime, considering battery lifetime, efficiency losses due to heating and cooling as well as capacity losses due to DoD and aging. Due to the selected functional units, the $NaNiCl_2$ battery can be compared with li-ion and lead-acid batteries.

To calculate the GWP_{100} over the whole life cycle, the individual processes were modelled with the software GaBi [42]. The exported results were used as an input for the generic LCA model of Stinder et al. et [17].

Life Cycle Inventory

The paper is prepared with support of a battery manufacturer. Any relevant information, such as a bill of materials (BOM) and manufacturing information, were shared with the

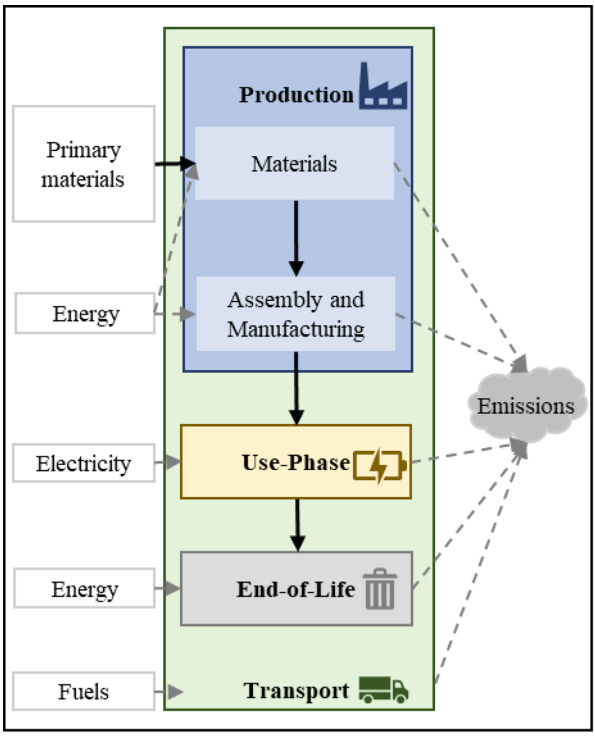

Fig. 4. System boundaries of the conducted LCA.

authors. Additionally, first-hand data from the mini grid in Tema were used. Hence, the quality of data can be considered as high.

Production

For the modelling of the production material composition, origin of the materials as well as processing of the materials are taken into consideration. Table 2 illustrates the aggregated material composition of the battery. In the material composition of the battery container, fumed silica, SiC and SiO_2 are mainly used for the thermal insulation material, while stainless steel is used for the frame. The largest share of the module's weight, 21.26 kg, is the stainless steel frame. The aluminium alloy is used for the BMS. The material "mica", known as glimmer, is the main component of the heater, which is necessary to achieve the operating temperature range. The 140 battery cells are the heaviest part of the battery with a weight of 344.21 kg. The separator, as illustrated in Fig. 2, is made of ceramic (Al_2O_3), the sacrificial electrode is made of aluminium, the melt of aluminium chloride and sodium chloride and the granulate is composed of different powders, like sodium chloride and nickel powder.

Most materials, measured by weight, come from Europe, whereby 46% come from Germany (DE), 24% from Switzerland and 24% from Great Britain (GB). 1% of the materials originate in China (CN), for 5% the country of origin is not known. For the modelling of the materials, we consider the respective electricity grid mix of the country

from which the material originates, as well as country-specific processes for the raw materials, depending on the availability in the GaBi database.

If processes or materials were not directly available in the database, we made reasonable assumptions based on literature and information from the producer, which are presented in detail below.

The insulation is provided by a vacuum insulation sheet. The core is made from silicon dioxide powder and silicon carbide, which are mixed and pressed to form a sheet. Together with fumed silica sheet the core is coated by a stainless steel foil. Afterwards the whole sheet is vacuumized. Mixing, pressing and vacuumizing requires energy. A LCA on vacuum insulation panels calculates an electricity demand of 1.0 kWh per m^2 [43]. Based on a weight of 5.5 kg per m^2, we calculate an energy demand of 0.106 kWh per kg vacuum sheet.

The energy demand for the rolling of the nickel cell case is modelled according to the energy demand of aluminium rolling, which requires 2.861 kWh per kg sheet. Ceramic components are made from aluminium oxide powder, which is cold-isostatic pressed (CIP) and sintered. The energy demand of CIP is - compared to sintering - negligible. Energy demand for sintering is modelled with 2.0 kWh per kg according to Çavdar [44]. When modelling the production of the glass paste, we estimated an thermal energy demand of 1.291 kWh per kg according to Fleischmann [45].

For stamping and bending of the closing cap made from nickel and for the positive electrode and the plug made from ferro-nickel, we consider an electricity demand of 0.049 kWh per kg as well as demand for compressed air and lubricating oil. For the punching of the sealing ring made from ferro-nickel, an electricity demand of 0.005 kWh per kg and the use of lubricating oil are accounted. The melt of aluminium chloride and sodium chloride is prepared by mixing and heating. We assume, it is melted in an oven for 1h at 150 °C, resulting a thermal energy demand of 2.4 kWh per kg, according to Hoppe et al. [46].

The granulate consists of several high quality powders. Nickel powder is produced in a carbonyl process, which results in a nickel powder with high purity. Due to the lack of data on the carbonyl process, we modelled the nickel powder process according to the atomisation of high purity (>99.8%) nickel as described by Vardelle et al. [47]. Nickel wires used in the process are made by a wiredrawing process with an electricity demand of 0.38 kWh per kg for melting and 0.34 kWh per kg for drawing. The following powderisation requires electricity of 0.38 kWh per kg for vacuum melting and 3.73 kg argon for gas atomisation. As the carbonyl process offers potential advantages regarding the energy demand and the usability of secondary material as input material, it is important to further research the nickel powder production in the future.

The atomisation of 1 kg iron powder needs approximately 10 L of water under pressure of 100 bar. Energy is required for melting, atomising and annealing of iron. The thermal energy consumption in powder production was examined to be 2.1 kWh per kg powder, according to Kruzhanov & Arnhold [48].

Aluminium powder is produced from high purity aluminium, obtained by electrolysis from aluminium oxide. Afterwards, the aluminium is atomised, requiring 2.25 kWh thermal energy per kg and 12.5 kg Argon per kg, as stated by Faludi et al. [49].

Table 2. Material composition of the battery.

	Component	**Materials**	**Weight**
Battery Container	Frame	Stainless steel	13.41 kg
	Insulation	Fumed silica, stainless steel, silicon dioxide (SiO_2), silicon carbide (SiC)	32.76 kg
	Plate	Stainless steel	0.25 kg
	Sealing	Rubber	0.01 kg
	Screws	Stainless steel	0.03 kg
	Ventilator	Stainless steel	0.09 kg
	Total		46.54 kg
Module	Mica Foil and Heater	Mica, coating	3.88 kg
	Frame	Stainless steel, nickel (Ni), PTFE, PE	25.13 kg
	Insulation	Fumed silica, stainless steel, silicon dioxide (SiO_2), silicon carbide (SiC)	10.20 kg
	BMS	Aluminium alloy, stainless steel, plastic, PCB	13.11 kg
	Total		52.33 kg
140 Battery cells	Cell case	Nickel	56.20 kg
	Ceramic components	Aluminium oxide (Al_2O_3)	49.84 kg
	Closing Cap	Nickel (Ni)	1.12 kg
	Glass paste	Glass powder, water and more	0.39 kg
	Granulate	Nickel powder, sodium chloride (NaCl), iron powder and more	133.07 kg
	Melt	Aluminium chloride (AlCl), sodium chloride (NaCl)	70.00 kg
	Electrode	Ferro-nickel	12.04 kg
	Neg. And pos. Cell connector	Steel	11.20 kg
	Sacrificial electrode	Aluminium	7.00 kg
	Plug	Ferro-nickel	0.28 kg
	Sealing Ring	Ferro-nickel	3.08 kg
	Total		344.21 kg
	Total Battery		443.08 kg

Sodium fluoride (NaF) powder is prepared by neutralizing hydrogen fluoride acid (HF) with sodium hydroxide (NaOH).

$$HF + NaOH \rightarrow NaF + H_2O \quad (1)$$

According to the stoichiometric relationship it requires 0.33 kg HF and 0.67 kg NaF to produce 0.3 kg H_2O and 0.6 kg NaF. To produce 1 kg NaF 1.492 kg of solvent NaF is needed. The water present in the solvent is then evaporated, requiring energy of 0.694 kWh per litre.

Sodium iodide (NaI) powder is produced by a reaction of sodium hydroxide (NaOH) with iodine (I_2).

$$6\ NaOH + 3\ I_2 \rightarrow 5\ NaI + NaIO_3 + 3\ H_2O \quad (2)$$

The mass of the reactants required to produce 1 kg NaI is calculated based on their stoichiometric relationship according to [50], who described the production of potassium iodide. The overall water demand amounts to 0.8 kg per kg sodium iodide. Furthermore, 0.478 kWh thermal energy per kg and 0.012 kWh electricity per kg are required to vaporize the resulting solvent and to operate a pressure filter. The GWP_{100} impact of iodine is considered, based on a characterization factor provided by Gong et al. [50] who calculated 4.66 kg CO_2eq per kg iodine.

Further processing and manufacturing are assumed to be carried out at the production site in Switzerland. Therefore, the factory specific electricity mix was considered. Around 56% of the electricity demand is generated by the company's own photovoltaic systems and the remaining amount from the Swiss electricity mix. For this purpose, the recent data sets were used in each case, with the electricity mixes from Switzerland being from 2018.

Transport

The emissions resulting from the transport of raw materials to the factory were calculated first. Therefore, the transport from DE, GB and CH to the factory was calculated exclusively via diesel trucks (EURO 0–6 mix). For the materials from China, the sea route with a container ship from Shenzhen (CN) to the port of Genova (IT) was considered, whereby the routes to the port in China and the routes to the factory in Switzerland are also covered by diesel trucks. For the filling of the diesel trucks, country-specific diesel mixes were chosen.

The transport of the final product to Ghana was also modelled by container ship, with the first and last meters being covered by truck.

Use Phase

The use phase of the battery is characterized by charging and discharging. The most important key indicator is how many kWh the battery discharges over its life cycle, meaning how many kWh of stored electricity can be used by the consumer. The considered battery has a usable capacity of 41 kWh and a life cycle usable capacity of 36.9, as explained in Sect.2.

The number of charging cycles and the lifetime of the battery are decisive for the total amount of electricity provided. In this paper, a distinction is made between two

Table 3. Lifetime assumptions of the battery.

	Scenario 1	Scenario 2
Nominal capacity	44.32 kWh	
Usable capacity	41.00 kWh	
Life cycle usable capacity	36.90 kWh	
Overall efficiency	85%	
Capacity loss factor	90%	
Charging cycles	4,500	3,500
Lifetime	15 years	10 years
kWh used over lifetime	166,050 kWh	129,150 kWh

scenarios. Scenario 1 assumes that about 4,500 charging cycles can be made over a period of 15 years. These assumptions are found in most literature [11]. Scenario 2 describes a more conservative experience-based scenario, in which about 3,500 charging cycles can be conducted over a period of 10 years. Table 3 summarizes the key numbers.

As already stated in Sect. 2, the battery does not need to be protected from external temperature by air conditioning or any similar means. However, the heater consumes a certain amount of the stored energy, which has already been subtracted from the overall efficiency. In this paper, the use-case in the mini grid is explored and compared to the use of li-ion and lead-acid batteries.

End-of-Life

As described in Sect. 2, there is no established recycling infrastructure for batteries in Ghana today. However, nickel recycling could be feasible with steel industry existing in Kumasi, Ghana. Therefore, two different scenarios are considered for the EoL treatment.

Scenario a: Shredding

For the first scenario, it is assumed the batteries are transported to a waste collection centre in Accra, where they are dismantled and shredded. However, only metallurgical processes, which are common in steel industry, are necessary for the recycling of $NaNiCl_2$ batteries. Therefore, the shredding scenario is unlikely and only included in the study to enhance comparability.

Scenario B: Recycling

Recycling refers to the further use of products or parts of products, which includes in particular material recycling, i.e. the reuse/recycling of materials [51]. In the case of the considered battery, the materials are not used for the production of new batteries after their EoL, but they are returned to the market and reused there. In the case of nickel for example, it is reused in the stainless steel industry [19]. Accordingly, it is an open-loop recycling, which is characterised by the fact that recycled materials from one product system are used in another product system and that the recycled material is modified in its inherent properties [40, 51].

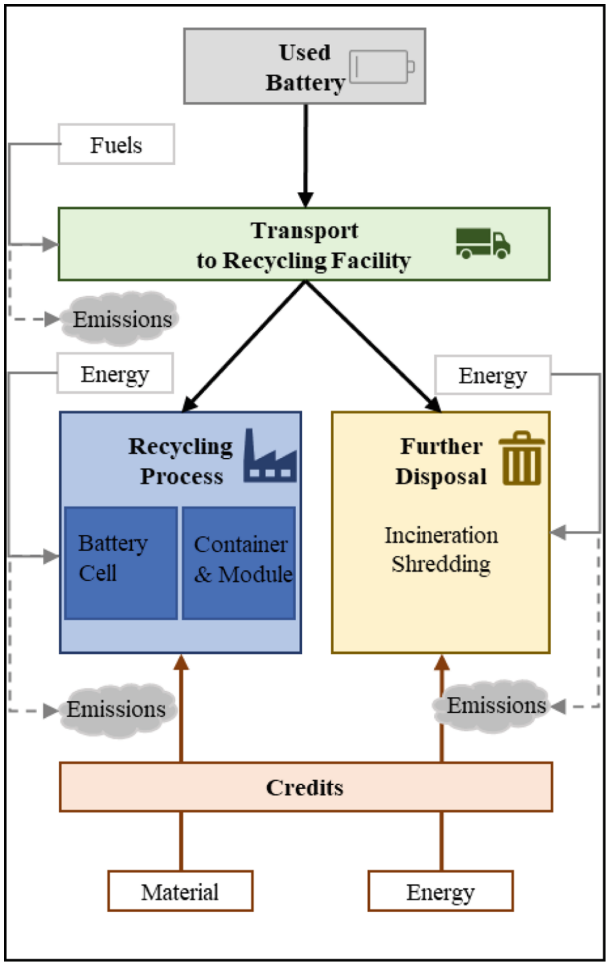

Fig. 5. Extension of system boundaries for EoL scenario 2 (Illustration and method based on Accardo et al. [15] and European Commission [52]).

The EoL option "recycling" in this study is modelled accordance with ISO 14044. It is based on the physical properties (mass) and does not consider economic values. For the recycling model, a system expansion is conducted, i.e. the system boundaries are shifted and include further product systems. The system expansion is implemented by counting credits for the utilization of the recycled materials in further product systems. As shown in Fig. 5, the recycling scenario includes transport, recycling processes and further disposal of the used battery. For the transport of the used battery to the recycling facility, fuels are used for truck and containership.

Credits are given for the second lifetime of the materials – used in another product system – and thermal energy and electricity recovered from the incineration process of plastics. While credits are given for the second use of the material and the energy,

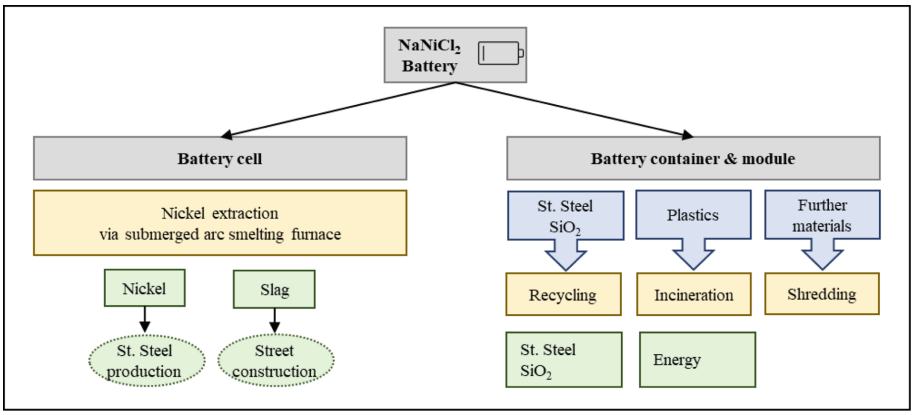

Fig. 6. Dismantling and recycling of the battery (Illustration based on European Commission [52]).

CO_2eq emissions resulting from the transport as well as the energy and resource demand for the recycling process, shredding and incineration process are also considered. We modelled that the batteries are transported to the steel industry in Kumasi, Ghana. For simplification, it is assumed that battery cells as well as the battery container and the module can be recycled there.

As there are very few studies about the recycling of $NaNiCl_2$ batteries, information provided by the manufacturer, by papers from Dustmann [19] and Galloway & Dustmann [53] are used to model the recycling of the battery. Figure 6 gives an overview on the dismantling and recycling process of the battery. In a first step, the battery cells are dismantled from the battery container and the module.

In our study, the main focus within the recycling of the battery cell is on nickel extraction [19, 53]. By heating the battery cells in submerged arc smelting furnace, the nickel can be extracted and used for stainless steel production. A slag, consisting of the ceramics, sodium and further leftover materials, remains, which can be used to replace limestone in road construction [53]. Submerged arc furnaces require a significant amount of electricity [54], which is included in the modelling of the recycling process.

The nickel makes up 128.76 kg, which are around 37% of the weight of the 140 battery cells (and 29% of the weight the total battery). According to the manufacturer around 95% of the nickel can be brought back to the market and a second lifetime in stainless steel industry can be established. By bringing the nickel back to the market, primary nickel is substituted. To calculate the recycling credit for nickel the following calculation is conducted.

The amount of replaced primary nickel material in a further product system (stainless steel production) is calculated by

$$0.95 * 128.76\,\text{kg} = 122.33\,\text{kg}. \tag{3}$$

To calculate the recycling credit for the nickel, let E_{Ni} be the GWP_{100} for primary nickel extraction for the 122.33kg, E_{En} be the $GWP_{100,}$ generated by the energy demand,

required in the recycling process of the battery cell, and E_{Tr} be the GWP_{100} of the transport to the recycling facility. Let also RC_{Ni} be the recycling credit for nickel recovery. Then the following

$$RC_{Ni} = E_{Ni} - E_{En} - E_{Tr} \tag{4}$$

applies. As the remaining slag is used in street construction as a replacement of limestone, the quality and purity of the material changed. Therefore, the recycling credit of the slag (RC_{Slag}), is calculated by:

$$RC_{Slag} = E_{Li} \tag{5}$$

whereby E_{Li} is the GWP_{100} for 221.89 kg of primary limestone production. E_{En} and E_{Tr} are not included in this recycling credit calculation, as they are already subtracted from the recycling credit for nickel. Furthermore, it is important to notice that GWP_{100} for limestone for construction is significantly lower than the former composition of the materials for the battery cell – keeping the credit for the usage of the slag small.

Inserting and calculating, results in

$$RC_{Ni} = 1,064.88\,\mathrm{kg}CO_2eq \tag{6}$$

and

$$RC_{Slag} = 1.15\,\mathrm{kg}CO_2eq. \tag{7}$$

As the transport of the battery is already included within the nickel recycling credit the transport will be neglected in the following paragraphs, to avoid double-counting. For the battery container and the module, it is assumed that stainless steel parts and SiO_2 are separated and prepared for recycling. As indicated in the publication on *Advances in ZEBRA batteries* [19], these materials are recycled and brought back to the market.

To determine the recycling credit for stainless steel recycling (RC_{St}), a paper from the Fraunhofer Institut IMW was considered [55]. By bringing stainless steel back to the raw material market, 4.3 kg CO_2eq can be saved per kg recycled steel [55]. As 45.27 kg stainless steel are contained in the battery's container and module, RC_{St} is calculated, as follows

$$RC_{St} = 45.27\,\mathrm{kg} * 4.3\,\mathrm{kg}CO_2eq/kg. \tag{8}$$

Hence, a credit of 194.65 kg CO_2eq is given for stainless steel recycling.

12.4 kg SiO_2 are comprised in the battery container and module. The recycling credit for SiO_2 recovery is indicated as RC_{SiO2}. As few data could be found on the recycling of SiO_2, a process for melting and conditioning glass with a share of 59% quartz was chosen as an approximation to simulate the necessary energy for the recycling process. By subtracting the emissions generated by the simulated process from the GWP_{100} for the extraction of primary SiO_2 - which is to be replaced in a further product system - the following value is obtained

$$RC_{SiO2} = 142.68\,\mathrm{kg}CO_2eq. \tag{9}$$

Furthermore, it is assumed that remaining plastic (0.53 kg) is incinerated. Therefore, corresponding waste incineration processes are selected in GaBi and credits resulting through upcoming thermal energy are taken into account. The overall emissions from the incineration (incl. The subtraction of credits given to regaining energy) are summarised in the factor E_{In}. Likewise, emissions coming from shredding all leftover components with a mass of 34.24 kg, are defined by the factor E_{Sh}.

This results in a total recycling credit of

$$RC = RC_{Ni} + RC_{Slag} + RC_{St} + RC_{SiO2} - E_{In} - E_{Sh}. \quad (10)$$

By entering the values, the sum makes up a total recycling credit of 1,401.76 kg CO_2eq.

4 Results

Corresponding to last two stages of the LCA methodology, this section presents the impact assessment and interpretation. This includes the depiction of the calculated GWP_{100} of the analysed $NaNiCl_2$ battery for the different life phases and components. Furthermore, we compare our results to the GWP_{100} of li-ion and lead-acid batteries.

The overall GWP_{100} caused by production, transport and EoL of the battery amounts to 2,931 kg CO_2eq (Scenario A). If we consider credits for the recycling, as described in the previous section, this results in a reduction of the GWP_{100} by 48%, thus 1,516 kg CO_2eq (Scenario B).

The absolute emissions over the battery lifetime are related to the functional unit one kWh electricity discharged and consumed, which is shown in Fig. 7. In Scenario 1-A, assuming a lifetime of 4,500 charging cycles, the battery causes 17.7 g CO_2eq per kWh consumed. This can be reduced by 48% if we consider recycling credits, resulting in a GWP_{100} of 9.1 g CO_2eq per kWh consumed. Scenario 2-A results in a 29% increased GWP_{100} compared to scenario 1-A due to the shorter battery lifetime of 3,500 charging cycles. In all scenarios the production phase contributes the majority of GWP_{100}, e.g. 98% in scenario 1-A.

Production Hot-Spots

Because of the high impact of the production phase, we examine the individual components and materials in more detail to identify hot-spots. Figure 8 depicts the share in weight and GWP_{100} of the three major battery components. The components account for approximately a similar proportion of the GWP_{100} as they do for the total weight of the battery. The largest share of 75% is caused by the battery cells, which we will present in more detail below. The majority of the GWP_{100} of the battery cell is caused by the production of the granulate (43%) and the cell case (35%) as shown in Fig. 9.

Major contributor within the granulate is the nickel powder. On the one hand it has a major weight share of 48% within the granulate and on the other hand it has a relatively high emission factor of 13.7 kg CO_2eq per kg nickel. The aluminium powder also causes relatively high specific emissions of 9.8 kg CO_2eq per kg aluminium, but it has a relatively low weight share in the granulate. Together nickel and aluminium

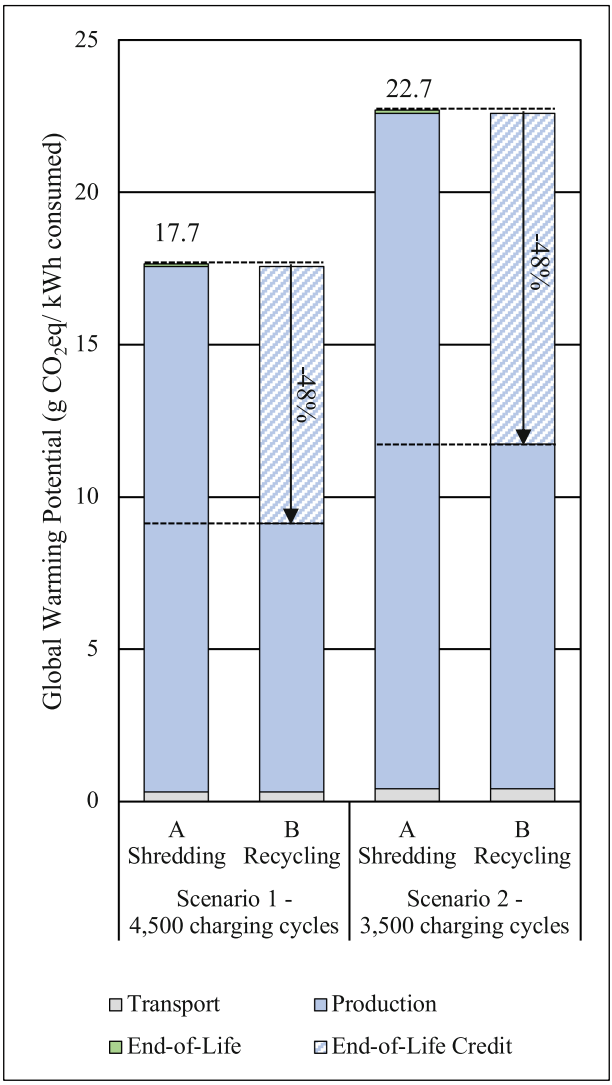

Fig. 7. Global Warming Potential of the analysed $NaNiCl_2$ batteries per kWh consumed for different scenarios regarding lifetime and EoL.

powder account for 98% of the GWP_{100} of the granulate. Similarly, the driving factor of the GWP_{100} of the cell case is the use of nickel as a material.

Comparison with Alternative Battery Types

To classify the results shown, we now compare them with the GWP_{100} of alternative battery technologies. Therefore, we choose the functional units one kWh nominal battery capacity, one kWh life cycle usable battery capacity and one kWh consumed as described in Sect. 3. The GWP_{100} for lead-acid and li-ion ($LiFePO_4$) batteries were obtained from

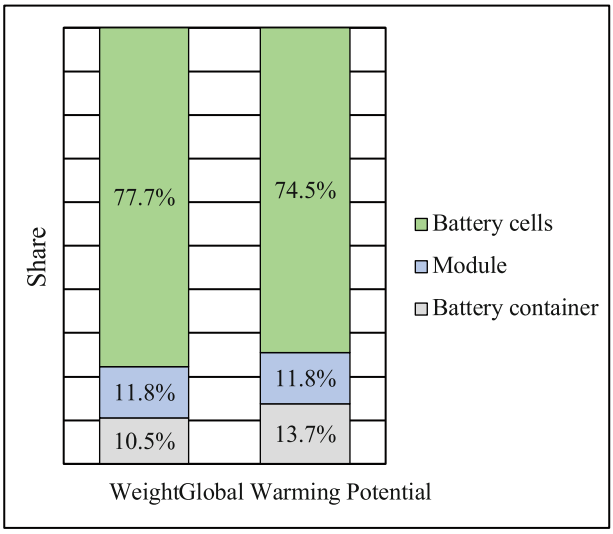

Fig. 8. Share of battery components in Global Warming Potential and weight.

the generic LCA model provided by Stinder et al. [17]. In this study, the GWP_{100} was calculated with the GaBi software and database.

Figure 10 compares the GWP_{100} of the three battery types per nominal and life cycle usable battery capacity. The comparison of GWP_{100} per nominal battery capacity shows that $NaNiCl_2$ batteries cause a 50% lower GWP_{100} per kWh than lead-acid batteries in the best case, i.e. with a long lifetime and the implementation of recycling. In comparison to li-ion batteries, the GWP_{100} is even 59% lower. However, if recycling cannot be implemented and we consider a shorter lifetime of 3,500 charging cycles, $NaNiCl_2$ batteries have a similar GWP_{100} per kWh like lead-acid batteries. Still, they would cause 22% lower emissions than li-ion batteries.

Now we compare the GWP_{100} per kWh of life cycle usable battery capacity, considering efficiency losses due to heating and cooling as well as capacity losses due to DoD and aging. The impact of the lead-acid battery is 183 kg CO_2eq per kWh life cycle usable battery capacity, compared to 69 kg CO_2eq per kWh nominal battery capacity. When comparing the life cycle usable capacity, the $NaNiCl_2$ battery has a 78% lower impact than the lead-acid battery in the best case and still 57% lower impact in the worst case. This is because lead-acid batteries have a lower DoD and therefore a lower usable capacity than $NaNiCl_2$ and li-ion batteries. Compared to li-ion batteries, the GWP_{100} per usable capacity of the $NaNiCl_2$ battery is 56% lower in the best case and 15% lower in the worst case.

Figure 11 depicts the GWP_{100} of the different battery types per kWh consumed, considering the electricity which can be discharged from the battery over its lifetime, taking into account efficiency and capacity losses. In the best case, the $NaNiCl_2$ battery has a 93% lower GWP_{100} than the lead-acid battery and a 71% lower GWP_{100} compared to the li-ion battery. In the worst case, the $NaNiCl_2$ battery still causes a 81% lower GWP_{100} than the lead-acid battery and 27% lower emissions than the li-ion battery. The

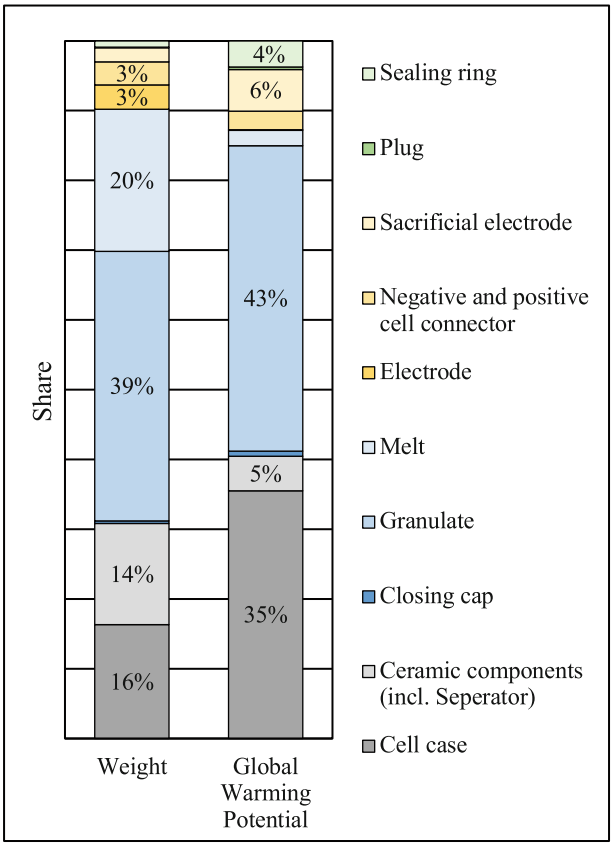

Fig. 9. Share of cell components in Global Warming Potential and weight.

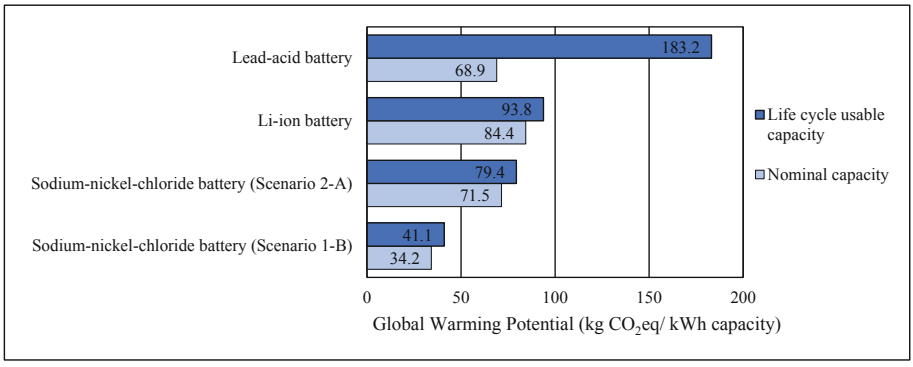

Fig. 10. Comparison of Global Warming Potential of different battery technologies per kWh battery capacity. The GWP_{100} of lead-acid and li-ion batteries is obtained from Stinder et al. [17].

comparatively high GWP_{100} of lead-acid batteries is due to their low usable capacity and short lifetime of 1,500 charge cycles compared to alternative battery technologies.

Use-Case: Don Bosco Mini Grid

The previously presented comparison with alternative battery types does not fully reflect their impact within application. Therefore, we will compare different configurations of the Don Bosco mini grid with various battery types below, based on the generic LCA model for mini grids of Stinder et al. [17]. Thereby, we also consider further mini grid installations like PV modules or inverters. The functional unit is one kWh of discharged and consumed energy. For the $NaNiCl_2$ batteries we consider the GWP_{100} of scenario 2-B which includes credits for recycling but assumes a shorter lifetime of 3,500 charging cycles.

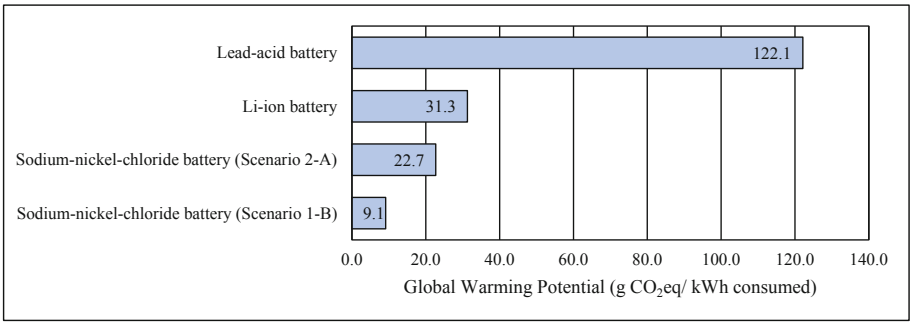

Fig. 11. Comparison of Global Warming Potential of different battery technologies per kWh consumed. The GWP_{100} of lead-acid and li-ion batteries is obtained from Stinder et al. [17].

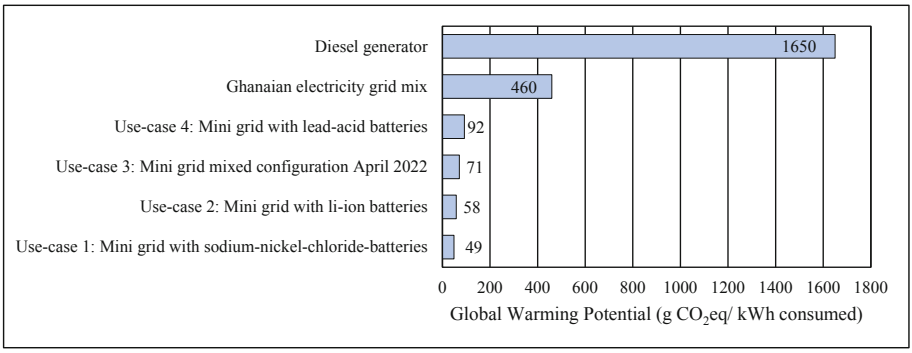

Fig. 12. Comparison of Global Warming Potential of electricity supply options in Ghana per kWh consumed. In use-case 3 37.6% of usable battery capacity is provided by lead-acid, 47.5% by li-ion and 14.9% by $NaNiCl_2$ batteries. The GWP_{100} of lead-acid and li-ion batteries is obtained from Stinder et al. [17]. The emission factor for the Ghanaian electricity mix is calculated according to the IGES List of Grid Emission Factors [56], for the Diesel generator it is based on German Environmental Agency [57].

The first use-case considers a hypothetical usage of only $NaNiCl_2$ batteries to replace all batteries in the Don Bosco mini grid. Considering a life cycle usable capacity of 36.90 kWh, 5.97 of these $NaNiCl_2$ batteries would be needed to replace the current usable battery capacity of 220.29 kWh. Under scenario 2, assuming a $NaNiCl_2$ battery lifetime of 10 years and roughly 3,500 cycles, 14.9 batteries are needed during the mini grid lifetime of 25 years. The first use-case results in a GWP_{100} of 49 g CO_2eq per kWh. In the second use-case, we consider the use of 15.9 li-ion batteries, each with a life cycle usable capacity of 13.86 kWh to replace the current available battery capacity, calculating a GWP_{100} of 58 g CO_2eq per kWh.

The third use-case analyses the actual configuration of the mini grid, as presented in Sect. 2, including 72 lead-acid batteries, eight li-ion batteries and one $NaNiCl_2$. This results in a GWP_{100} of 71 g CO_2eq per kWh. A fourth use-case considers the hypothetical usage of only lead-acid batteries to replace all batteries in the Don Bosco mini grid. Considering a life cycle usable capacity of 1.37 kWh per lead-acid battery, 160.8 batteries would be needed to replace the current usable battery capacity, resulting in a GWP_{100} of 92 g CO_2eq per kWh.

Figure 12 compares the GWP_{100} of the different mini grid configurations to the Ghanaian electricity grid mix and a diesel generator. All mini grid configurations achieve a significant emission reduction compared to the Ghanaian grid mix and the diesel generator. The first use-case, a mini grid based solely on $NaNiCl_2$ batteries, reduces the GWP by 89% in comparison to the Ghanaian grid and by 97% compared to the diesel generator. The third use-case, the mixed mini grid configuration, reduces the GWP by 84% compared to the grid mix and by 96% compared to a diesel generator. Compared to the third use-case (mixed configuration) the first use-case (only $NaNiCl_2$ batteries) reduces the GWP_{100} by 32%.

5 Conclusion and Discussion

In this study, we determined that the GWP_{100} of $NaNiCl_2$ batteries is 9.1 g CO_2eq per kWh consumed in the best case, when the battery has a long lifetime of 4,500 charging cycles and nickel, steel and silicon dioxide are recycled at EoL. Our worst case, i.e., assuming a 22% shorter lifetime and no recycling, results in a GWP_{100} of 22.7 g CO_2eq per kWh consumed. The GWP_{100} of the production phase of the $NaNiCl_2$ battery is dominated by nickel materials. Therefore, nickel recycling offers great added value in terms of the environmental impact of $NaNiCl_2$ batteries and should be enforced and incentivized by policy measures.

Overall, we could highlight that $NaNiCl_2$ batteries could decrease the GWP_{100} per kWh consumed over lifetime by up to 93% compared to lead-acid and up to 71% compared to li-ion batteries. The major advantages compared to lead-acid batteries can be attributed to a longer lifetime and a higher usable capacity. A further advantage of $NaNiCl_2$ batteries compared to li-ion and lead-acid batteries is a lower consumption of toxic and rare materials. This not only improves the recyclability of $NaNiCl_2$ batteries, but also simplifies their production. Thus, manufacturers of $NaNiCl_2$ batteries state that the setup of production facilities requires lower investment costs than for li-ion batteries and could already be competitive even with small-scale production. Unlike li-ion

batteries, $NaNiCl_2$ batteries do not require "giga-factories". Therefore, it would also be feasible to produce the batteries directly in the country of use.

However, at present $NaNiCl_2$ batteries still have higher costs than li-ion and lead-acid batteries. The economic advantages can only be realized with upscaling of production capacities. In addition, $NaNiCl_2$ batteries are not suitable for all applications. The charging current of $NaNiCl_2$ battery is limited by the endothermic charging reaction. While li-ion batteries can be charged with a current of 0.5 C, $NaNiCl_2$ batteries need to be charged with a current of about C 5, otherwise the temperature of the cell could cool down below the minimal operation temperature. This makes them unsuitable for fast charging. Discharge currents between li-ion and $NaNiCl_2$ batteries are similar. Overall, when selecting the optimum battery technology, it is always necessary to consider other parameters, such as the battery's energy density, weight, and volume, as well as the requirements of the use-case. Mobile applications in vehicles, or stand-by applications for example, require different battery characteristics than the analysed use-case in a mini grid.

Further research on the environmental impact of $NaNiCl_2$ batteries should focus on additional impact categories, like depletion of resources as well as human and eco toxicity, to validate their advantages compared to alternative battery types. Additionally, it would be valuable to assess their costs and recyclability in detail. To improve the reliability of our conducted LCA, we recommend researching the recycling of $NaNiCl_2$ batteries based on a financial allocation in the future. Furthermore, uncertain parameters like battery lifetime should be analysed in a further sensitivity analysis. Moreover, a validation of data on energy demand in manufacturing would be valuable. Especially the carbonyl process to produce nickel powder offers potential advantages regarding the energy demand and the usability of secondary material as input material and should be further investigated.

The Laboratory for Sustainable Technologies plans to research further applications of the $NaNiCl_2$ batteries, e.g. in urban solar-based charging infrastructure for mobility. Within a real-world laboratory, part of the research project SCiSusMob, different charging infrastructure options with batteries are to be tested. The aim is to collect data for their ecological, technical, and economic evaluation and optimization. The results of the conducted LCA will also be used in the MoNaL project, in which the Don Bosco mini grid is researched and optimized.

Acknowledgments. Research was funded by quality improvement funds of Bochum University of Applied Sciences. Data sets used in this research were funded by the German Federal Ministry of Education and Research within the project SCiSusMob, grant number 13FH0I73IA. Data on battery characteristic and manufacturing were kindly provided by the company Battery Consult. We thank Brent Hendrickx for assistance with literature recommendations for the life cycle inventory of the battery.

Authors' Contributions. Malina Nikolic: Methodology, Formal analysis, Investigation, Data Curation, Writing - Original Draft, Visualization; Nora Schelte: Conceptualization, Validation, Writing - Original Draft, Visualization; Michele Velenderic; Validation, Resources, Writing - Original Draft; Frederick Adjei: Investigation, Writing - Original Draft; Semih Severengiz: Supervision, Funding acquisition, Writing - Review & Editing.

References

1. J. Rockström, O. Gaffney, J. Rogelj, M. Meinshausen, N. Nakicenovic, and H. J. Schellnhuber, "A roadmap for rapid decarbonization," *Science*, vol. 355, no. 6331, pp. 1269–1271, Mar. 2017, doi: https://doi.org/10.1126/science.aah3443.
2. IEA, "Renewables 2021 - Analysis and forecast to 2026," 2021, [Online]. Available: https://iea.blob.core.windows.net/assets/5ae32253-7409-4f9a-a91d-1493ffb9777a/Renewables2021-Analysisandforecastto2026.pdf
3. D. A. Quansah, M. S. Adaramola, and L. D. Mensah, "Solar Photovoltaics in Sub-Saharan Africa – Addressing Barriers, Unlocking Potential," *Energy Procedia*, vol. 106, pp. 97–110, Dec. 2016, doi: https://doi.org/10.1016/j.egypro.2016.12.108.
4. "The Role of Energy Storage for Mini-Grid Stabilization," *IEA-PVPS*. https://iea-pvps.org/key-topics/the-role-of-energy-storage-for-mini-grid-stabilization/ (accessed Jul. 28, 2022).
5. "Off-grid renewable energy systems: Status and methodological issues," */publications/2015/Feb/Off-grid-renewable-energy-systems-Status-and-methodological-issues*. https://www.irena.org/publications/2015/Feb/Off-grid-renewable-energy-systems-Status-and-methodological-issues (accessed Jul. 28, 2022).
6. S. AMDC Energy Limited, "Battery Energy Storage Systems." http://www.amdcenergy.com/markets-services/energy-strorage/battery-energy-storage-systems.html (accessed Aug. 08, 2022).
7. H. C. Hesse, M. Schimpe, D. Kucevic, and A. Jossen, "Lithium-Ion Battery Storage for the Grid—A Review of Stationary Battery Storage System Design Tailored for Applications in Modern Power Grids," *Energies*, vol. 10, no. 12, Art. no. 12, Dec. 2017, doi: https://doi.org/10.3390/en10122107.
8. R. Weidl, M. Schulz, M. Hofacker, H. Dohndorf, and M. Stelter, "Low cost, ceramic battery components and cell design," Freiberg, Germany, 2016, p. 020004. doi: https://doi.org/10.1063/1.4961896.
9. P. Kurzweil, "HISTORY | Secondary Batteries," in *Encyclopedia of Electrochemical Power Sources*, J. Garche, Ed. Amsterdam: Elsevier, 2009, pp. 565–578. doi: https://doi.org/10.1016/B978-044452745-5.00004-6.
10. R. Manzoni, "Sodium Nickel Chloride batteries in transportation applications," in *2015 International Conference on Electrical Systems for Aircraft, Railway, Ship Propulsion and Road Vehicles (ESARS)*, Mar. 2015, pp. 1–6. doi: https://doi.org/10.1109/ESARS.2015.7101491.
11. EASE, "Sodium-Nickel-Chloride Battery," *EASE Storage*, 2022. https://ease-storage.eu/energy-storage/technologies/ (accessed Jul. 29, 2022).
12. N. Shamim, E. C. Thomsen, V. V. Viswanathan, D. M. Reed, V. L. Sprenkle, and G. Li, "Evaluating ZEBRA Battery Module under the Peak-Shaving Duty Cycles," *Materials*, vol. 14, no. 9, p. 2280, Apr. 2021, doi: https://doi.org/10.3390/ma14092280.
13. S. Longo, V. Antonucci, M. Cellura, and M. Ferraro, "Life cycle assessment of storage systems: the case study of a sodium/nickel chloride battery," *J. Clean. Prod.*, vol. 85, pp. 337–346, Dec. 2014, doi: https://doi.org/10.1016/j.jclepro.2013.10.004.
14. S. Longo *et al.*, "Life Cycle Assessment for Supporting Eco-Design: The Case Study of Sodium–Nickel Chloride Cells," *Energies*, vol. 14, no. 7, Art. no. 7, Jan. 2021, doi: https://doi.org/10.3390/en14071897.
15. A. Accardo, G. Dotelli, M. L. Musa, and E. Spessa, "Life Cycle Assessment of an NMC Battery for Application to Electric Light-Duty Commercial Vehicles and Comparison with a Sodium-Nickel-Chloride Battery," *Appl. Sci.*, vol. 11, no. 3, Art. no. 3, Jan. 2021, doi: https://doi.org/10.3390/app11031160.
16. D. Ou, "State of the art of Life Cycle Inventory data for electric vehicle batteries," p. 46.

17. A. K. Stinder, S. Finke, M. Vendeleric, and S. Severengiz, "A generic GHG-LCA model of a smart mini grid for decision making using the example of the Don Bosco mini grid in Tema, Ghana," *Procedia CIRP*, vol. 105, pp. 776–781, Jan. 2022, doi: https://doi.org/10.1016/j.procir.2022.02.129.
18. H. Sakaebe, "ZEBRA Batteries," in *Encyclopedia of Applied Electrochemistry*, G. Kreysa, K. Ota, and R. F. Savinell, Eds. New York, NY: Springer, 2014, pp. 2165–2169. doi: https://doi.org/10.1007/978-1-4419-6996-5_437.
19. C.-H. Dustmann, "Advances in ZEBRA batteries," *J. Power Sources*, vol. 127, no. 1–2, pp. 85–92, Mar. 2004, doi: https://doi.org/10.1016/j.jpowsour.2003.09.039.
20. Kompetenznetzwerk Lithium-Ionen-Batterien e. V., "Natrium-Nickelchlorid-Batterie - Batterieforum Deutschland." https://www.batterieforum-deutschland.de/infoportal/lexikon/natrium-nickelchlorid-batterie/ (accessed Aug. 13, 2022).
21. D. L. Thompson *et al.*, "The importance of design in lithium ion battery recycling – a critical review," *Green Chem.*, vol. 22, no. 22, pp. 7585–7603, 2020, doi: https://doi.org/10.1039/D0GC02745F.
22. A. Väyrynen and J. Salminen, "Lithium ion battery production," *J. Chem. Thermodyn.*, vol. 46, pp. 80–85, Mar. 2012, doi: https://doi.org/10.1016/j.jct.2011.09.005.
23. A. Nedjalkov *et al.*, "Toxic Gas Emissions from Damaged Lithium Ion Batteries—Analysis and Safety Enhancement Solution," *Batteries*, vol. 2, no. 1, Art. no. 1, Mar. 2016, doi: https://doi.org/10.3390/batteries2010005.
24. M. Bilharz, "Lithium-Batterien und Lithium-Ionen-Akkus," *Umweltbundesamt*, Jan. 22, 2015. https://www.umweltbundesamt.de/umwelttipps-fuer-den-alltag/elektrogeraete/lithium-batterien-lithium-ionen-akkus (accessed Jul. 28, 2022).
25. Y. Chen *et al.*, "A review of lithium-ion battery safety concerns: The issues, strategies, and testing standards," *J. Energy Chem.*, vol. 59, pp. 83–99, Aug. 2021, doi: https://doi.org/10.1016/j.jechem.2020.10.017.
26. J. Hou, M. Yang, D. Wang, and J. Zhang, "Fundamentals and Challenges of Lithium Ion Batteries at Temperatures between −40 and 60 °C," *Adv. Energy Mater.*, vol. 10, no. 18, p. 1904152, 2020, doi: https://doi.org/10.1002/aenm.201904152.
27. I. A. Bergdahl and S. Skerfving, "Chapter 19 - Lead." https://reader.elsevier.com/reader/sd/pii/B9780128229460000362?token=95984B2D3EAE10379E3FAD9DC47BFE0CC856A071AAFC7062DE2159A42CF74FCCC156E70273883403AA48AF9230024C2B&originRegion=eu-west-1&originCreation=20220728102631 (accessed Jul. 28, 2022).
28. K. Owusu-Sekyere, A. Batteiger, R. Afoblikame, G. Hafner, and M. Kranert, "Assessing data in the informal e-waste sector: The Agbogbloshie Scrapyard," *Waste Manag.*, vol. 139, pp. 158–167, Feb. 2022, doi: https://doi.org/10.1016/j.wasman.2021.12.026.
29. B. Ericson *et al.*, "The Global Burden of Lead Toxicity Attributable to Informal Used Lead-Acid Battery Sites," *Ann. Glob. Health*, vol. 82, no. 5, pp. 686–699, Sep. 2016, doi: https://doi.org/10.1016/j.aogh.2016.10.015.
30. G. J. May, A. Davidson, and B. Monahov, "Lead batteries for utility energy storage: A review," *J. Energy Storage*, vol. 15, pp. 145–157, Feb. 2018, doi: https://doi.org/10.1016/j.est.2017.11.008.
31. L. Gaines, "The future of automotive lithium-ion battery recycling: Charting a sustainable course," *Sustain. Mater. Technol.*, vol. 1–2, pp. 2–7, Dec. 2014, doi: https://doi.org/10.1016/j.susmat.2014.10.001.
32. R. Christensen, "Na-NiCl2 batteries," *Technol. Data Energy Storage*, pp. 147–160, 2018.
33. I. S. S. Pinto, "Separation and recovery of nickel, as a salt, from an EDTA leachate of spent hydrodesulphurization catalyst using precipitation methods," *Chem. Eng. Sci.*, p. 9, 2015.
34. World Bank, "Access to electricity (% of population) - Ghana | Data," 2022. https://data.worldbank.org/indicator/EG.ELC.ACCS.ZS?locations=GH (accessed May 09, 2022).

35. S. Chaaraoui *et al.*, "Day-Ahead Electric Load Forecast for a Ghanaian Health Facility Using Different Algorithms," *Energies*, vol. 14, no. 2, p. 409, Jan. 2021, doi: https://doi.org/10.3390/en14020409.
36. "Ghana - Countries & Regions," *IEA*. https://www.iea.org/countries/ghana (accessed May 13, 2022).
37. A. Yadoo and H. Cruickshank, "The role for low carbon electrification technologies in poverty reduction and climate change strategies: a focus on renewable energy mini-grids with case studies in Nepal, Peru and Kenya.," *Energy Policy*, vol. 42, pp. 591–602, 2012.
38. B. Tenenbaum, C. Greacen, T. Siyambalapitiya, and J. Knuckles, "From the Bottom Up : How Small Power Producers and Mini-Grids Can Deliver Electrification and Renewable Energy in Africa," World Bank, Washington, DC, Jan. 2014. Accessed: Jul. 28, 2022. [Online]. Available: https://openknowledge.worldbank.org/handle/10986/16571
39. International Organization for Standardization, "ISO 14040:2006," *ISO*. https://www.iso.org/cms/render/live/en/sites/isoorg/contents/data/standard/03/74/37456.html (accessed Aug. 14, 2022).
40. International Organization for Standardization, "ISO 14044:2006," *ISO*. https://www.iso.org/cms/render/live/en/sites/isoorg/contents/data/standard/03/84/38498.html (accessed Aug. 14, 2022).
41. P. Foster *et al.*, "Changes in Atmospheric Constituents and in Radiative Forcing," in *Climate Change 2007: The Physical Science Basis. Contribution of Working Group I to the Fourth Assessment Report of the Intergovernmental Panel on Climate Change*, Cambridge, United Kingdom and New York: Cambridge University Press, 2007, pp. 130–234
42. Sphera Solutions GmbH, "Professional database 2022," 2022. https://gabi.sphera.com/support/gabi/gabi-database-2022-lci-documentation/professional-database-2022/ (accessed Jul. 14, 2022).
43. S. Resalati, T. Okoroafor, P. Henshall, N. Simões, M. Gonçalves, and M. Alam, "Comparative life cycle assessment of different vacuum insulation panel core materials using a cradle to gate approach," *Build. Environ.*, vol. 188, p. 107501, Jan. 2021, doi: https://doi.org/10.1016/j.buildenv.2020.107501.
44. uğur çavdar, "Energy Consumption Analysis of Sintering Temperature Optimization of Pure Aluminum Powder Metal Compacts Sintered by Using The UHFIS," *Uluslar. Muhendislik Arastirma Ve Gelistirme Derg.*, pp. 174–185, Dec. 2017, doi: https://doi.org/10.29137/umagd.348072.
45. Fleischmann, Bernhard, "Neuer Ansatz zur Bilanzierung des Energieeinsatzes bei der Glaserstellung und der Versuch der geschlossenen Darstellung von Kennzahlen aus der Produktionstechnik und aus statistischen (Wirtschafts-) Daten," *Dgg J.*, vol. 17, no. 3, pp. 11–22, 208AD.
46. A. Hoppe *et al.*, "Sodium Solid Electrolytes: NaxAlOy Bilayer-System Based on Macroporous Bulk Material and Dense Thin-Film," *Materials*, vol. 14, no. 4, p. 854, Feb. 2021, doi: https://doi.org/10.3390/ma14040854.
47. A. Vardelle, A. Moign, Jean-Gabriel Legoux, and N. J. Themelis, "Life Cycle Assessment - a Comparison of Various Thermal Spray Processes and Electroplating," 2009, doi: https://doi.org/10.13140/RG.2.1.1059.0480.
48. V. Kruzhanov and V. Arnhold, "Energy consumption in powder metallurgical manufacturing," *Powder Metall.*, vol. 55, no. 1, pp. 14–21, Feb. 2012, doi: https://doi.org/10.1179/174329012X13318077875722.
49. J. Faludi, M. Baumers, I. Maskery, and R. Hague, "Environmental Impacts of Selective Laser Melting: Do Printer, Powder, Or Power Dominate?," *J. Ind. Ecol.*, vol. 21, no. S1, Nov. 2017, doi: https://doi.org/10.1111/jiec.12528.

50. J. Gong, S. B. Darling, and F. You, "Perovskite photovoltaics: life-cycle assessment of energy and environmental impacts," *Energy Environ. Sci.*, vol. 8, no. 7, pp. 1953–1968, 2015, doi: https://doi.org/10.1039/C5EE00615E.
51. G. Fleischer, *Aufwands- und ergebnisrelevante Probleme der Sachbilanzierung*. Jülich: Forschungszentrum, Zentralbibliothek, 2002.
52. European Comission (EC), "PEFCR - Product Environmental Footprint Category Rules for High Specific Energy Rechargeable Batteries for Mobile Applications," 2018. https://ec.europa.eu/environment/eussd/smgp/pdf/PEFCR_Batteries.pdf (accessed Aug. 23, 2022).
53. D. R. C. Galloway, M.-D. Sa, V. Laveggio, and S. Switzerland, "ZEBRA Battery - Material Cost Availability and Recycling," p. 9.
54. Y. Yang, Y. Xiao, and M. A. Reuter, "Analysis of Transport Phenomena in Submerged Arc Furnace for Ferrochrome Production," p. 12.
55. Fraunhofer IMW, "Schrottbonus Konkret." https://www.imw.fraunhofer.de/content/dam/moez/de/documents/211124_Schrottbonus%20Konkret_BDSV.pdf (accessed Aug. 24, 2022).
56. Institute for Global Environmental Strategies, "List of Grid Emission Factors version 10.10," 2021. https://pub.iges.or.jp/pub/iges-list-grid-emission-factors
57. Kristina Juhrich, "Climate Change. CO2 Emission Factors for Fossil Fuels," German Environment Agency (UBA), 2016.